Supporting Information

Alkyl Chain Engineering of Chlorinated Acceptors for Elevated Solar Conversion

Daize Mo,[‡,a,b] Hui Chen,[‡,a, c] Jiadong Zhou,[‡,d] Ningning Tang,[d] Liang Han,[a] Yulin Zhu,[a] Pengjie Chao,[a] Hanjian Lai,[a] Zengqi Xie*[,d] and Feng He*[,a]

[a] Shenzhen Grubbs Institute and Department of Chemistry, Southern University of Science and Technology, Shenzhen 518055, China.

[b] Institute of Chinese Medical Sciences, University of Macau, Macao 999078, China.

[c] Academy for Advanced Interdisciplinary Studies, Southern University of Science and Technology, Shenzhen 518055, China

[d] Institute of Polymer Optoelectronic Materials and Devices, State Key Laboratory of Luminescent Materials and Devices, South China University of Technology, Guangzhou 510640, China.

[‡]These authors contributed equally to this work.

*E-mail: hef@sustech.edu.cn (F.H.); msxiez@scut.edu.cn (Z.X.)

1. General Methods

Characterization: ^{1}H NMR spectra were obtained using a Bruker AV-500 spectrometer in deuterated chloroform solution at room temperature with tetramethylsilane (TMS) as the internal reference. The following abbreviations were used for signal multiplicities: s, singlet; d, doublet; t triplet; m, multiple. Preparative gel permeation chromatography purification was performed with a JAI LC-9104 recycling preparative high-performance liquid chromatography, and the eluent was chloroform. The molecular mass was confirmed by using an Autoflex III matrix-assisted laser desorption ionization mass spectrometer (MALDI-TOF-MS). Thermogravimetric analysis (TGA) plots were conducted on a Discovery series instrument under a nitrogen atmosphere with a heating rate of 10 ℃ /min in N_2. UV-Vis absorption spectra were recorded on the Shimadzu UV3600 spectrometer. Cyclic voltammetry was performed on a Model CHI 660E potentiostat / galvanostat (Shanghai Chenhua Instrumental Co., Ltd. China) to determine the HOMO and LUMO levels of the monomers, in an dichloromethane solution of 0.1 mol L^{-1} tetrabutylammoniumhexafluorophosphate (*n*-Bu_4NPF_6) at a potential scan rate of 100 mV s^{-1} with an Ag/Ag+ reference electrode and a platinum wire counter electrode under an argon atmosphere. The redox potential of ferrocene/ferrocene^{+} (Fc/Fc^{+}) under the same conditions is located at 0.044 V, which is assumed to have an absolute energy level of -4.8 eV to vacuum. The HOMO and LUMO were calculated by the following equation: HOMO (eV)=-4.74+ φ_{ox}, LUMO (eV)=-4.74+φ_{red}.Whereφ_{ox} is the onset oxidation potential *vs* Ag/Ag+ and φ_{red} is the onset reduction potential vs

Ag/Ag^{+}. Atom force microscopy (AFM) images were taken on a NanoScope IIIa controller (Veeco Metrology Group / Digital Instruments, Santa Barbara, CA, USA), using built-in software (version V6.13R1) to capture images. Transmission electron microscopy (TEM) images were acquired using a HITACHI H-7650 electron microscope operating at an acceleration voltage of 100 kV. The **BTIC-BO-4Cl** crystal data was analyzed by the Mercury software (CCDC Software Ltd). Each crystal cell was constituted two kind of **BTIC-BO-4Cl** in two different directions (both with four molecules), which were labeled in blue and green, respectively. If the single crystal unit grow and stack along a, b, and c axis for 2.5 times, the crystal packing diagrams of **BTIC-BO-4Cl** will get when observe from the direction of the crystal plane which were intersects with the ac axis.

Device Fabrication and Testing: The ITO substrates were sonicated sequentially in acetone, detergent, deionized water and isopropyl alcohol to clean the ITO surface, followed by drying at 90 ℃ for overnight in vacuum oven. ZnO interlayer from precursor solution was spin-coated onto the pre-cleaned and UV-treated ITO substrates, and then heated at 200 ℃ for 1 hour. The device structures of ITO/ZnO/PBDB-TF: chlorinated acceptors/MoO_3/Ag was fabricated. The polymers were co-dissolved in $CHCl_3$, at total solids concentration of 4 mg mL^{-1}, the solutions were stirred overnight at temperature of 70 ℃. When using chlorobenzene as the process solvents, PBDB-TF: **BTIC-EH-4Cl** (D/A, 1:1.2) and PBDB-TF: **BTIC-BO-4Cl** (D/A, 1:1.2) were dissolved in chlorobenzene at the PBDB-TF concentration of 9 mg mL^{-1}. The active layer solutions should be stirred at 40˚C for

over 3h. Before spin-coating the active layer, 0.5% 1,8-diiodooctane (v/v) was added to the solutions. The active layer was spin-coated from the cooled blend solution obtain high neat films, part of them were treated by thermal annealing at 100 ℃. Subsequently, the resulted active films were transferred into a vacuum chamber. Afterwards, 10 nm molybdenum oxide (MoO_3) hole buffer and 100 nm Ag electrode was deposited by thermal evaporation through a defined shadow mask in a vacuum chamber with a pressure of approximately 1×10^{-4} Pa. The completed devices were tested in closed glove box.

Characterization of device: Steady-state current-voltage (*J*-*V*) curves were measured by a Keithley 2400 source-measurement unit under AM 1.5 G spectrum from a solar simulator (Enli Technology Co., Ltd., Taiwan) calibrated by a silicon reference cell (Hamamatsu S1133 color, with KG-5 visible fifth). All EQE data were gained through the measurement of solar cell spectral response measurement system QE-R3011 (Enli Technology Co., Ltd., Taiwan). The mobility of electron was tested by fitting the current-bias characteristics in dark utilizing a field-independent space charge limited current (SCLC) model following the Mott-Gurney law. Hole-only devices were fabricated with the device structure ITO/PEDOT:PSS/PBDB-TF: chlorinated acceptors/MoO_3/Ag. The mobility was determined by fitting the dark current to the model of a single carrier SCLC, which is described by the equation

$$J = \frac{9}{8}\varepsilon_0\varepsilon_r\mu_h\frac{V^2}{d^3}$$

where J is the current, μ_h is the zero-field mobility, ε_0 is the permittivity of free space, ε_r is the relative permittivity of the material, d is the thickness of the active layer, and

V is the effective voltage. The effective voltage can be obtained by subtracting the built-in voltage (V_{bi}) and the voltage drop (V_s) from the substrate's series resistance from the applied voltage (V_{appl}), $V = V_{appl} - V_{bi} - V_{s.}$ The hole-mobility can be calculated from the slope of the $J^{1/2}$- V curves.

2. Materials and synthesis

4,7-dibromo-benzo[c][1,2,5]thiadizole, fuming nitric acid, fuming sulfuric acid, sulfuric acid, 3-bromothiophene, dodecanoyl chloride, AlCl3, ethyl thioglycolate, copper power, quinolone, bis(triphenylphosphine)palladiumm(II)dichloride ($PdCl_2(PPh_3)_2$), tri-*n*-butyltinchloride ((n-Bu)$_3$SnCl), *n*-butyllithium (*n*-BuLi), and triphenylphosphine (PPh_3) were purchased from Shanghai Macklin Biochemical Co., Ltd. and used without further purification. All other reagents and chemicals were purchased from commercial sources and used without further purification unless stated otherwise. PBDB-TF (M_n= 49 kDa) was obtained from Solarmer Energy Inc. Tetrahydrofuran (THF) and toluene were freshly distilled prior to use under nitrogen protection dried over Na/benzophenone. **4b** was purchased from the Derthon Optoelectrinic Materials Science Technology Co (Shenzhen, China). 2-(5,6-dichloro-3-oxo-2,3-dihydro-1H-inden-1-ylidene)malononitrile, 3-undecylthieno[3,2-b]-thiophene, and 4,7-dibromo-5,6-dinitrobenzo[c][1,2,5]thiadiazole were synthesized according to the previously reported procedures.

Synthesis of Compound 1. Tributyl(6-undecylthieno[3,2-b]thiophene-2-yl)stannane was synthesized according to our previous method. After that, the product was used in the next procedure directly without further purification. Briefly,

tributyl(6-undecylthieno[3,2-b]thiophene-2-yl)stannane, 4,7-dibromo-5,6-dinitro-benzo[c][1,2,5]thiadiazole and $Pd(PPh_3)Cl_2$ were dissolved in 100 mL of toluene in a 250 mL round bottom flask under the protection of dry argon. The reaction was stirred at 80 ℃ overnight, then cooled to room temperature and concentrated under reduced pressure. The title compound (**1**) was purified by column chromatography on a silica gel column (dichloromethane/petroleum ether (1/3, v/v)) as a red solid (13.75 g, 84.8% yield). ^{1}H NMR (400 MHz, $CDCl_3$) δ: 7.74 (s, 2H), 7.20 (s, 2H), 2.79(t, *J* = 8Hz, 4H), 1.86-1.76 (m, 4H), 1.66-1.65 (m, 4H), 1.42-1.16 (m, 16H), 0.91-0.81(m, 16H).

Synthesis of Compound 2. In a 250 mL round bottomed flask, compound **1** (13.75 g, 16.975 mmol), PPh_3 (44.39 g, 169.75 mmol), and o-dichlorobenzene (100 mL) were added and refluxed at 185 ℃ overnight. After that, remained solvent was distilled under the reduced pressure and then subjected to silica gel column chromatographic separation using hexane/dichloromethane (1/1) and then dichloromethane to yield **2** as the red solid (15.24 g, > 100%). The product was used directly into the following reaction without further purification.

Synthesis of Compound 3a. A mixture of compound **2** (4.22 g, 5.647 mmol), sodium hydroxide (2.25 g, 56.48 mmol), 1-Bromododecane (12.33 mL, 51.45 mmol), and 60 mL DMF was refluxed at 90 ℃ for 15 h. The solvent was removed by rotary evaporation, and the residue was purified with column chromatography on silica gel column chromatography with petroleum ether/dichloromethane (10/1) as the eluent to yield **3a** as a red solid (3.11 g).^{1}H NMR (400 MHz, $CDCl_3$) δ: 7.01 (s, 2H), 4.61 (t, *J* = 8 Hz, 4H), 2.82 (t, *J* = 8 Hz, 4H), 2.07 (t, *J* = 8 Hz, 2H).Due to the existence of the

1-bromododecane, so the other alkyl chain peaks we have not mark them here. Here, the crude product was used directly to the next procedure without further purification. MS (MALDI) calcd for $C_{64}H_{98}N_4S_5$ [M+]: 1082. 6395. Found: 1082.588.

Synthesis of Compound 3c. Synthesis of **3c** was carried out in a similar manner to that of **3a**. ^{1}H NMR (400 MHz, $CDCl_3$) δ: 7.01 (s, 2H), 4.69 (d, *J* = 8 Hz, 4H), 2.83 (t, *J* = 8 Hz, 4H), 2.10-2.04 (m, 2H), 1.89-1.83 (m, 4H), 1.40-1.27 (m, 68H), 0.90-0.81(m, 30H), 0.68-0.51 (m, 14H). MS (MALDI) calcd for $C_{64}H_{98}N_4S_5$ [M+]: 1082. 6395. Found: 1082.587.

Synthesis of Compound 3d. Synthesis of **3d** was carried out in a similar manner to that of **3a**.^{1}H NMR (400 MHz, $CDCl_3$) δ: 7.01 (s, 2H), 4.60 (d, *J* = 8 Hz, 4H), 2.82 (t, *J* = 8 Hz, 4H), 2.07 (t, *J* = 8 Hz, 2H), 1.89-1.82 (m, 4H), 1.45-1.31 (m, 58H), 1.19-1.12(m, 8H), 1.03-0.91 (m, 22H), 0.90-0.88 (m, 25H), 0.84-0.66 (m, 16H). MS (MALDI) calcd for $C_{72}H_{114}N_4S_5$ [M+]: 1194.7467. Found: 1194.772.

Synthesis of Compound 4a. To a solution of compound **3a** (1.1 g, 1.01 mmol) in $ClCH_2CH_2Cl$ (30 mL) and DMF (5 mL) at 0 ℃, phosphorous oxychloride (1.46 mL, 15.72 mmol) was added slowly under the protection of argon. After stirring at 0 ℃ for 1 h and then refluxed at 90 ℃ overnight. The reaction mixture was poured into deionized water (150 mL) and then extracted with dichloromethane three times. The combined organic layer was washed with water, dried over $NaSO_4$, and the solvents were distilled under reduced pressure. The residue was purified by silica gel column chromatograph, using petroleum ether/dichloromethane (1/1, v/v) as the eluent to give **4a** as a red solid (1 g, 86.95% yield). ^{1}H NMR (400 MHz, $CDCl_3$) δ: 10.11 (s, 2H),

4.64 (t, *J* = 8 Hz, 4H), 3.18 (t, *J* = 8 Hz, 4H), 1.95-1.90 (m, 8H), 1.37-1.27 (m, 8H), 1.26-1.12 (m, 92H), 0.85 (t, *J* = 8 Hz, 4H).^{13}C NMR (100 MHz, $CDCl_3$) δ: 181.71, 147.24, 145.81, 143.12, 136.89, 136.65, 131.69, 129.18, 127.16, 112.43, 50.99, 31.91, 31.89, 31.12, 30.32, 29.65, 29.62, 29.57, 29.45, 29.38, 29.34, 29.31, 29.10, 28.12, 26.54, 22.69. MS (MALDI) calcd for $C_{64}H_{98}N_4O_2S_5$ [M+]: 1138.6293. Found: 1138.619.

Synthesis of Compound 4c. Synthesis of **4c** was carried out in a similar manner to that of **4a**. ^{1}H NMR (400 MHz, $CDCl_3$) δ: 10.15 (s, 2H), 4.64 (d, *J* = 8 Hz, 4H), 3.21 (t, *J* = 8 Hz, 4H), 2.04 (t, *J* = 4 Hz, 2H), 1.51-1.43 (m, 4H), 1.38 (d, *J* = 8 Hz, 4H), 1.09-0.77 (m, 42H), 0.80-0.59 (m, 14H).^{13}C NMR (100 MHz, $CDCl_3$) δ: 181.72, 147.49, 145.86, 143.17, 137.04, 136.81, 132.96, 132.94, 129.66, 112.29, 55.25, 38.87, 31.91, 31.50, 30.35, 30.31, 30.18, 30.02, 29.64, 29.60, 29.52, 29.28, 29.33, 28.16, 27.91, 27.73, 25.21, 25.00, 22.73, 22.69, 22.44, 22.42, 14.12, 13.94, 13.92, 13.71, 13.68. MS (MALDI) calcd for $C_{64}H_{98}N_4O_2S_5$ [M+]: 1138.6293. Found: 1138.595.

Synthesis of Compound 4d. Synthesis of **4d** was carried out in a similar manner to that of **4a**. ^{1}H NMR (400 MHz, $CDCl_3$) δ: 10.17 (s, 2H), 4.65 (d, *J* = 8 Hz, 4H), 3.22 (t, *J* = 8 Hz, 4H), 2.07-1.99 (m, 2H), 1.97-1.91 (m, 4H), 1.54-1.40 (m, 5H), 1.43-1.29 (m, 40H), 1.23-1.14 (m, 8H), 1.05-0.88 (m, 50H), 0.86-0.68 (m, 24H).^{13}C NMR (100 MHz, $CDCl_3$) δ: 181.74, 147.49, 145.83, 143.18, 137.03, 136.78, 137.99, 129.66, 127.45, 112.39, 55.22, 38.88, 31.91, 31.76, 31.53, 30.37, 30.30, 29.69, 29.66, 29.65, 29.60, 29.52, 29.38, 29.34, 29.29, 29.12, 28.17, 25.40, 25.34, 22.69, 22.58, 22.47, 14.12, 14.11, 13.95. MS (MALDI) calcd for $C_{72}H_{114}N_4O_2S_5$ [M+]: 1250.7545. Found:

1250.795.

Synthesis of Compound BTIC-C12-4Cl.Compound **4a** (0.19 g, 0.166 mmol) and 2-(5, 6-dichloro-3-oxo-2,3-dihydro-1H-inden-1-ylidene)malononitrile (0.175 g, 0.666 mmol) were added to a 25 mL round bottom flask. After the flask was blanked by argon three times, chloroform (25 mL) and pyridine (0.5 mL) was added, and then the mixture was stirred at 70 ℃ overnight. After cooling to room temperature, the product was precipitated via the addition of 200 mL of methanol and filtered. The crude product was purified with column chromatography on silica gel using $CHCl_3$ as the eluent to give a dark blue solid **BTIC-C12-4Cl** (0.144 g, 53.1% yield). ^{1}H NMR (400 MHz, $CDCl_3$) δ: 8.44 (s, 2H), 8.34 (s, 2H), 7.62 (s, 2H), 4.45 (m, 4H), 2.74 (t, J = 8 Hz, 4H), 2.08 (m, 4H), 1.03 (d, J = 8 Hz, 8H), 1.54-1.49 (m, 32H), 1.40-1.39 (m, 14H), 1.22-1.14(m, 88H), 0.82-0.73 (m, 20H). ^{13}C NMR (100 MHz, $CDCl_3$) δ: 185.53, 156.55, 153.84, 146.51, 144.98, 139.02, 138.46, 138.07, 136.75, 135.21, 133.74, 132.67, 131.59, 130.11, 119.11, 114.35, 112.92, 69.05, 51.17, 31.99, 31.95, 30.42, 30.20, 30.11, 30.01, 29.92, 29.86, 29.72, 29.63, 29.54, 29.43, 29.39, 27.03, 22.75, 22.70, 14.18, 14.08. MS (MALDI) calcd for $C_{90}H_{102}Cl_4N_8O_2S_5$ [M+]: 1628.5454. Found: 1628.126.

Synthesis of Compound BTIC-EH-4Cl. Synthesis of **BTIC-EH-4Cl** was carried out in a similar manner to that of **BTIC-C12-4Cl**. Due to the limited solubility of **BTIC-EH-4Cl**, we have not provided its ^{13}C NMR here. ^{1}H NMR (400 MHz, $CDCl_3$) δ: 9.18 (s, 2H), 8.79 (s, 2H), 7.98 (s, 2H), 4.78 (d, *J* = 8 Hz, 4H), 3.24 (t, J = 8 Hz, 4H), 2.05-2.12 (m, 2H), 1.92-1.84 (m, 4H), 1.51 (d, *J* = 8 Hz, 4H), 1.37(t, J = 8 Hz,

4H), 1.28 (d, *J* = 4 Hz, 30H), 1.18-1.14 (m, 5H), 1.07-0.94 (m, 14H), 0.87 (t, J = 8 Hz, 8H), 0.71-0.64 (m, 14H). MS (MALDI) calcd for $C_{82}H_{86}Cl_4N_8O_2S_5$ [M+]: 1516.4202. Found: 1516.096.

Synthesis of Compound BTIC-BO-4Cl. Synthesis of **BTIC-BO-4Cl** was carried out in a similar manner to that of **BTIC-C12-4Cl**. ^{1}H NMR (400 MHz, $CDCl_3$) δ: 9.17 (s, 2H), 8.79 (s, 2H), 7.96 (s, 2H), 4.78 (d, *J* = 8 Hz, 4H), 3.23 (t, J = 8 Hz, 4H), 2.14-2.12 (m, 2H), 1.91-1.86 (m, 4H), 1.51 (d, *J* = 8 Hz, 4H), 1.37(t, J = 8 Hz, 4H), 1.28 (d, *J* = 4 Hz, 32H), 0.87 (t, J = 8 Hz, 10H), 0.71-0.64 (m, 14H). ^{13}C NMR (100 MHz, $CDCl_3$) δ:186.13, 158.57, 154.04, 147.43, 145.31, 139.43, 139.14, 138.71, 137.71, 136.36, 136.02, 135.63, 134.25, 133.60, 131.15, 126.84, 124.91, 119.84, 115.06, 114.58, 113.65, 68.71, 55.80, 39.25, 31.92, 31.64, 31.21, 30.55, 30.43, 29.84, 29.66, 29.62, 29.52, 29.45, 29.35, 28.07, 27.93, 14.13, 14.07, 13.81, 13.78. MS (MALDI) calcd for $C_{90}H_{102}Cl_4N_8O_2S_5$ [M+]: 1628.5454. Found: 1628.353.

Synthesis of Compound BTIC-HD-4Cl. Synthesis of **BTIC-HD-4Cl** was carried out in a similar manner to that of **BTIC-BO-4Cl**. ^{1}H NMR (400 MHz, $CDCl_3$) δ: 9.19 (s, 2H), 8.80 (s, 2H), 7.92 (s, 2H), 4.77 (d, *J* = 8 Hz, 4H), 3.23 (t, J = 8 Hz, 4H), 2.13-2.10 (m, 2H), 1.90-1.84 (m, 4H), 1.37(t, *J*= 8 Hz, 4H),1.28-1.26 (m, 38H), 1.13 (t, *J* = 8 Hz, 18H), 1.01 (s, 36H), 0.87 (t, *J*=8 Hz, 12H), 0.79 (t, *J*=8 Hz, 10H), 0.68 (t, *J*=6 Hz, 8H). ^{13}C NMR (100 MHz, $CDCl_3$) δ: 185.09, 158.55, 154.93, 147.48, 145.30, 139.47, 139.12, 138.70, 137.66, 136.38, 136.01, 135.60, 134.32, 133.61, 131.23, 126.84, 124.89, 119.81, 115.05, 114.58, 113.63, 68.71, 55.75, 39.28, 31.93, 31.87, 31.66, 31.22, 30.67, 29.88, 29.84, 29.67, 29.63, 29.53, 29.45, 29.43, 29.36, 29.24,

25.72, 25.63, 22.70, 22.64, 22.54, 14.13, 14.08. MS (MALDI) calcd for $C_{98}H_{118}Cl_4N_8O_2S_5$ [M+]: 1741.6739. Found: 1741.513.

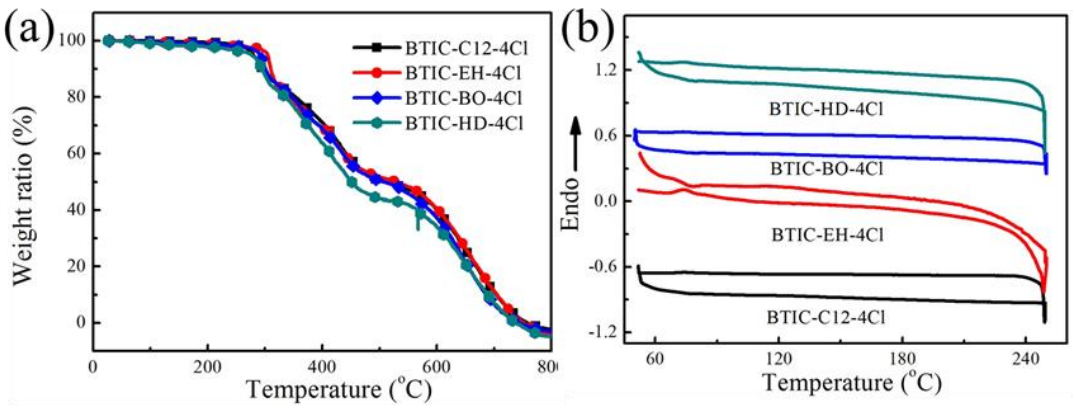

Figure S1. Thermogravimetric analysis (a), and differential scanning calorimetry (b) of four acceptors.

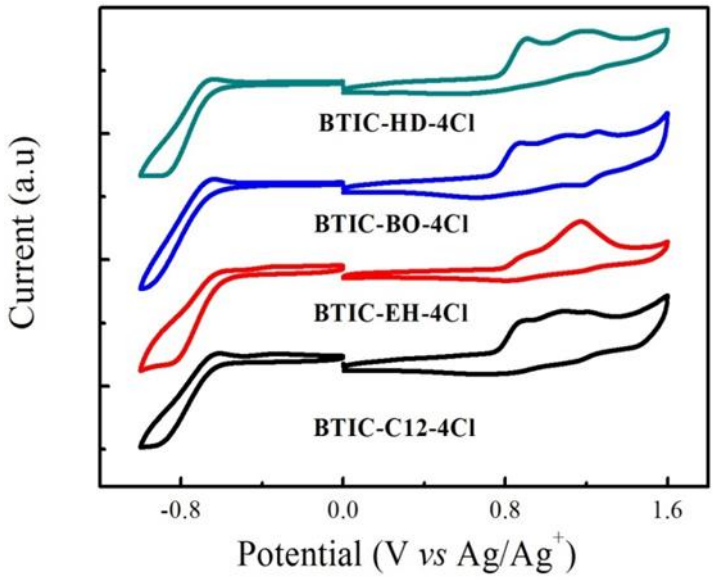

Figure S2. Cyclic voltammograms of four acceptors in dichloromethane solution with $(n\text{-}Bu)_4NPF_6$ (0.1 M) as the electrolyte.

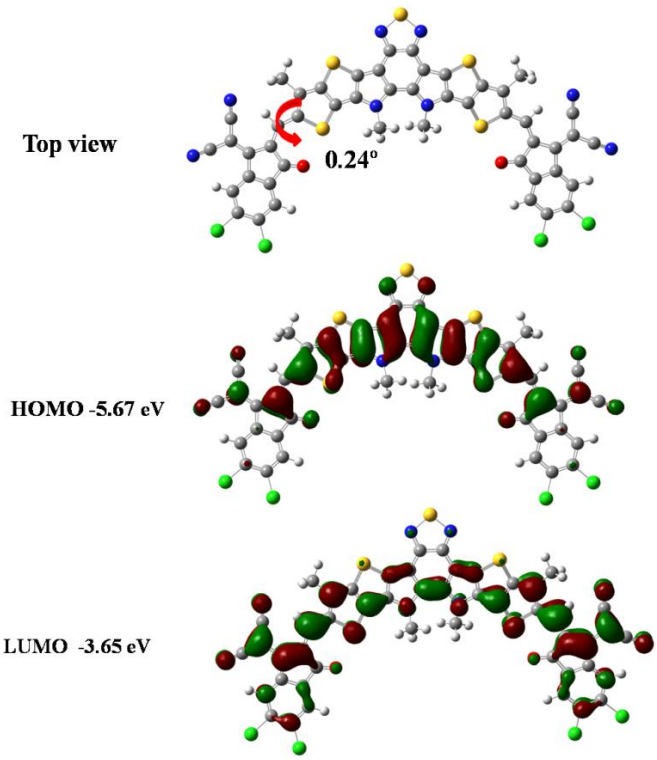

Figure S3. Optimized geometries and calculated molecular orbital of the chlorinated acceptors.

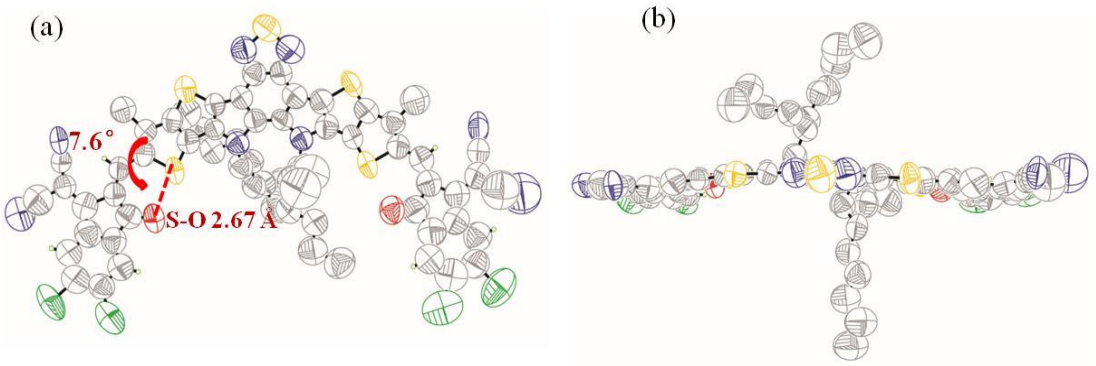

Figure S4. Single crystal structure of **BTIC-BO-4Cl** (2-butyloctyl and n-undecyl side chains were neglected for clarity). (a) Top view. (b) Side view.

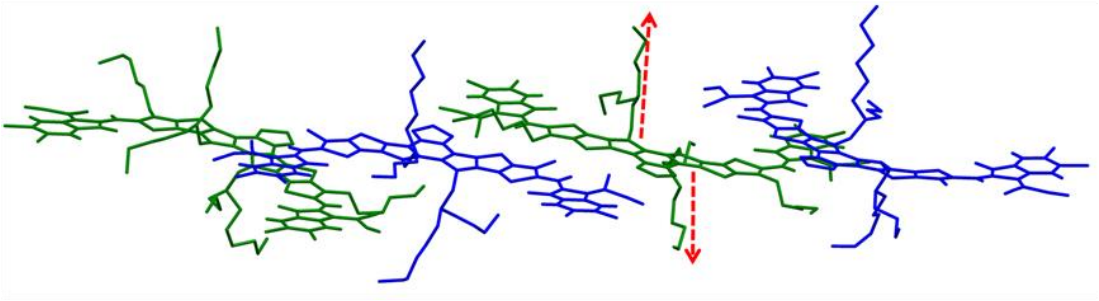

Figure S5. X-ray crystal structures of the **BTIC-BO-4Cl** acceptors.

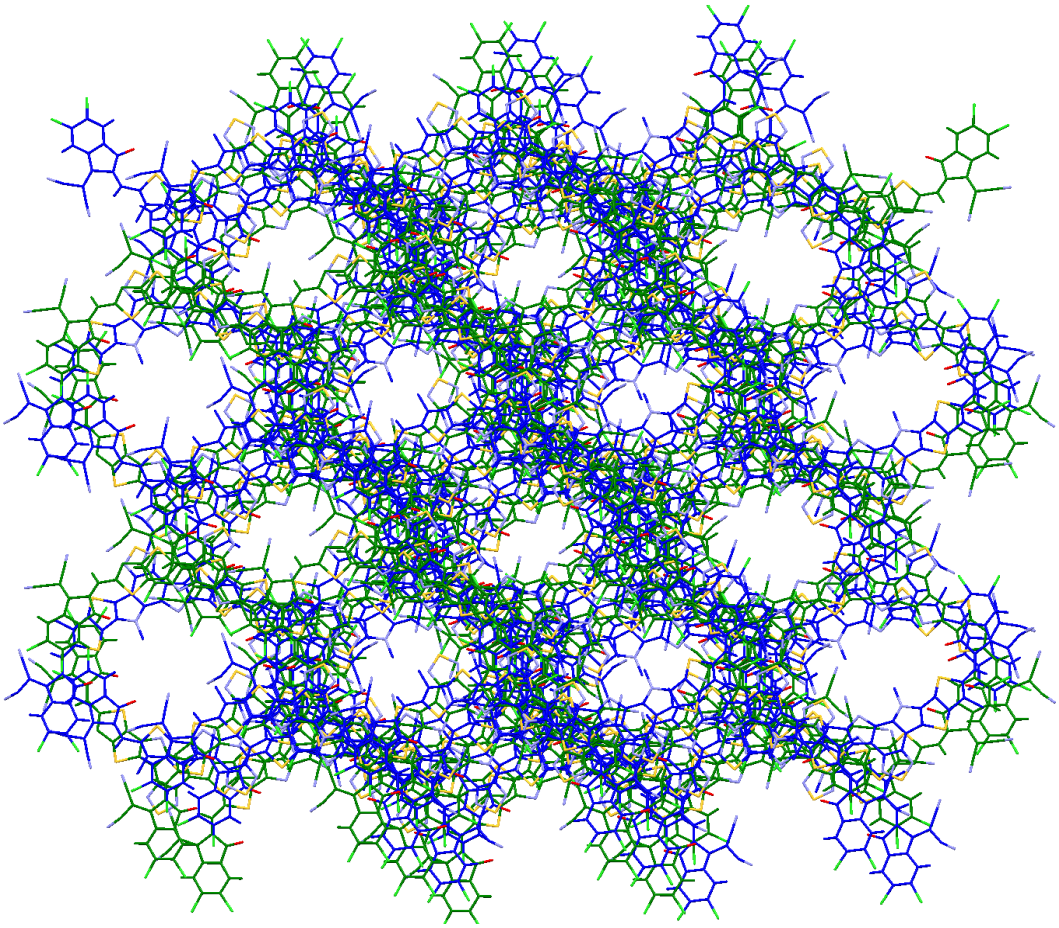

Figure S6. Crystal packing diagrams of **BTIC-BO-4Cl** (2-butyloctyl and n-undecyl side chains were neglected for clarity).

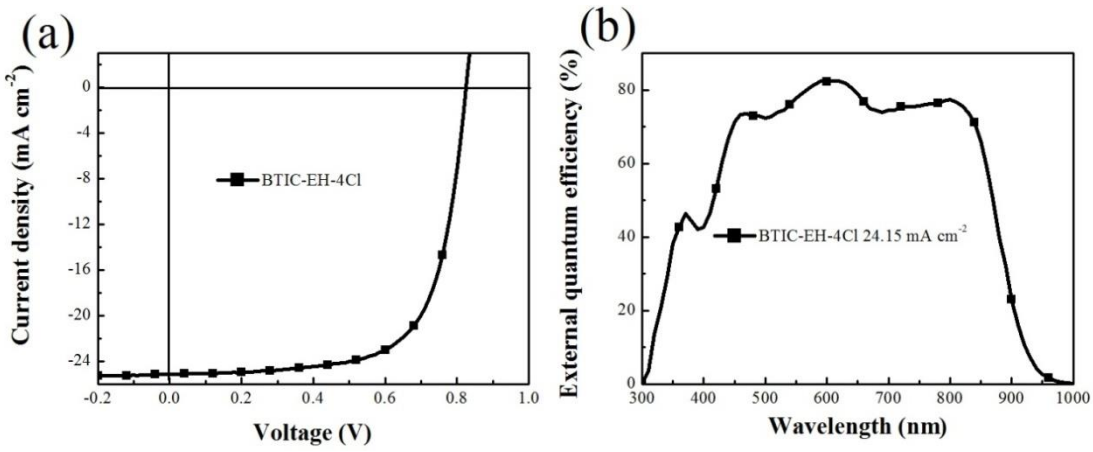

Figure S7. (a) *J-V* curves of the OSCs based on **BTIC-EH-4Cl**: PBDB-TF when processed from chlorobenzene; (b) EQE spectra of the devices.

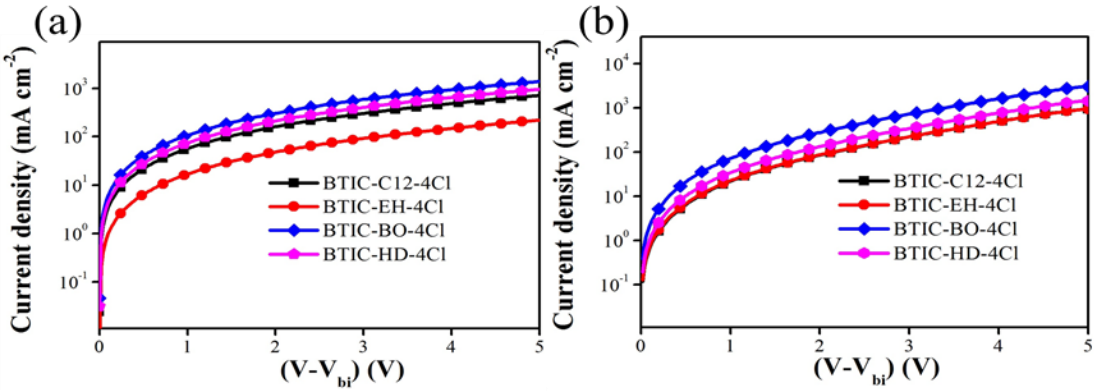

Figure S8. The *J-V* curves of the hole-only (a) and electron-only (b) of **BTIC-C12-4Cl**, **BTIC-EH-4Cl**, **BTIC-BO-4Cl**, and **BTIC-HD-4Cl**-based devices.

Table S1. Extracted mobility of the chlorinated acceptors.

Acceptors	Hole Mobility ($cm^2 v^{-1} s^{-1}$)	Electron Mobility ($cm^2 v^{-1} s^{-1}$)	Hole Mobility / Electron Mobility
BTIC-C12-4Cl	1.9×10^{-4}	8.7×10^{-5}	2.2
BTIC-EH-4Cl	5.7×10^{-5}	7.7×10^{-5}	0.74
BTIC-BO-4Cl	3.6×10^{-4}	2.4×10^{-4}	1.5
BTIC-HD-4Cl	2.5×10^{-4}	1.1×10^{-4}	2.3

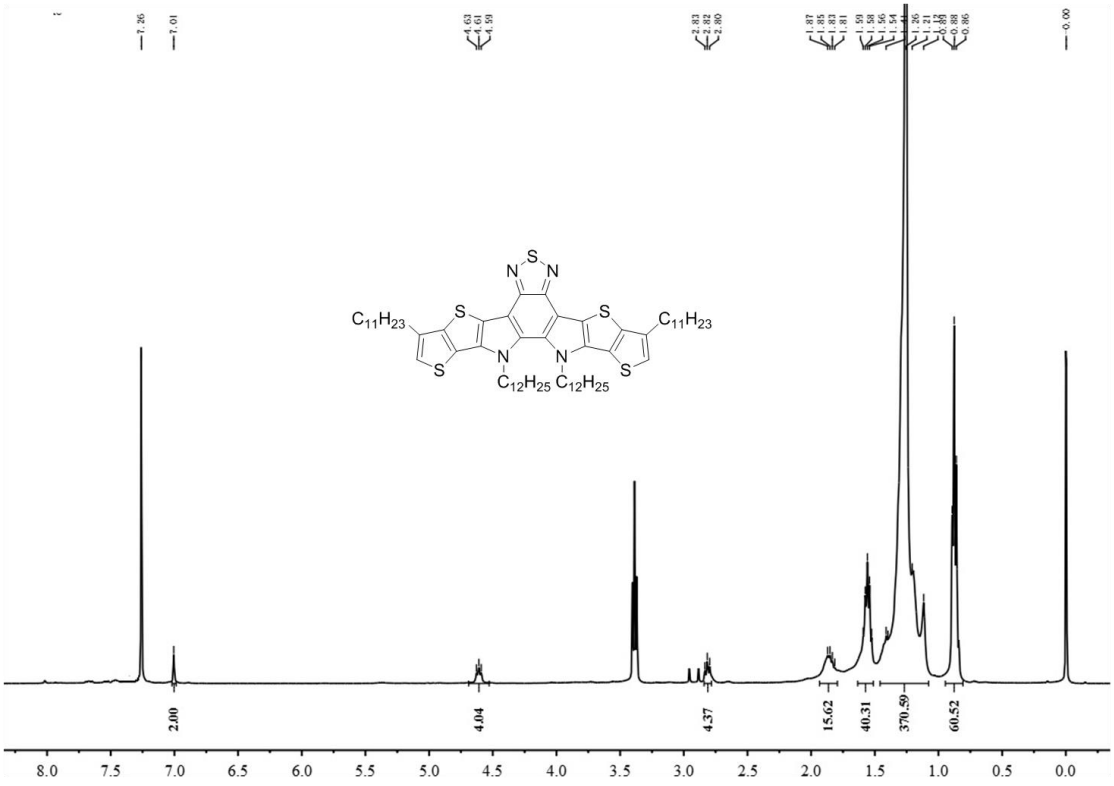

Figure S9. ^{1}H NMR spectrum of **3a** in $CDCl_3$.

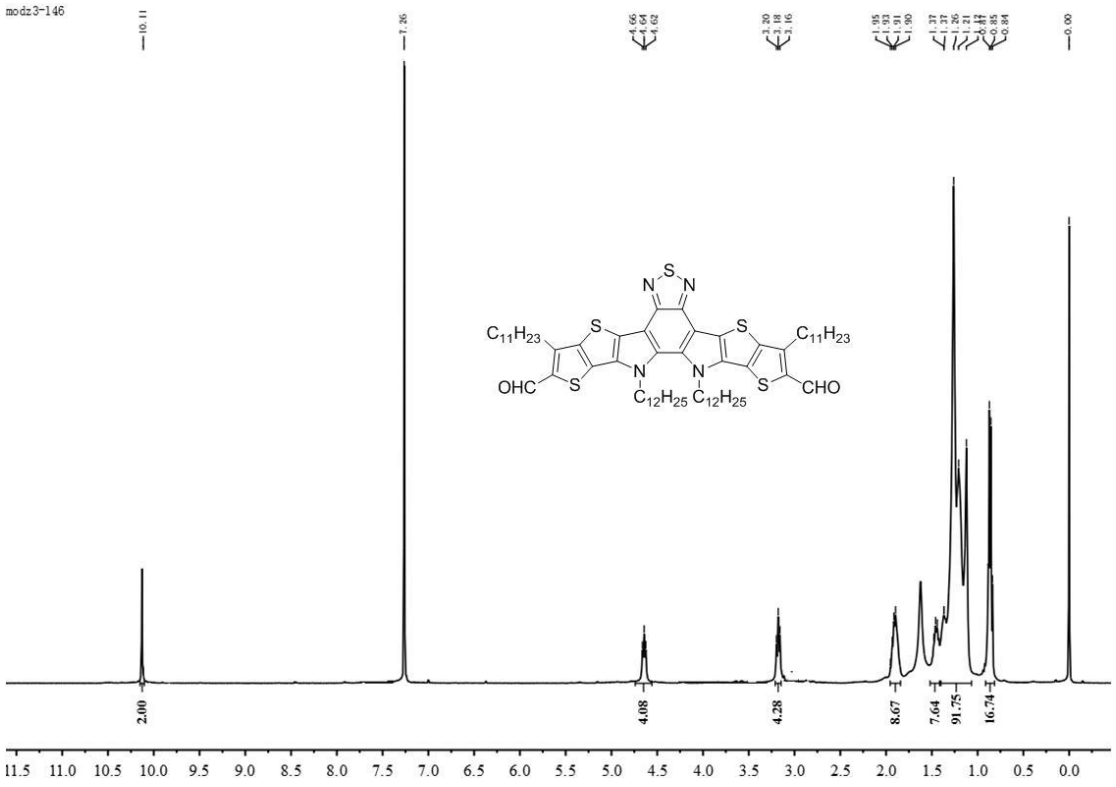

Figure S10. ^{1}H NMR spectrum of **4a** in $CDCl_3$.

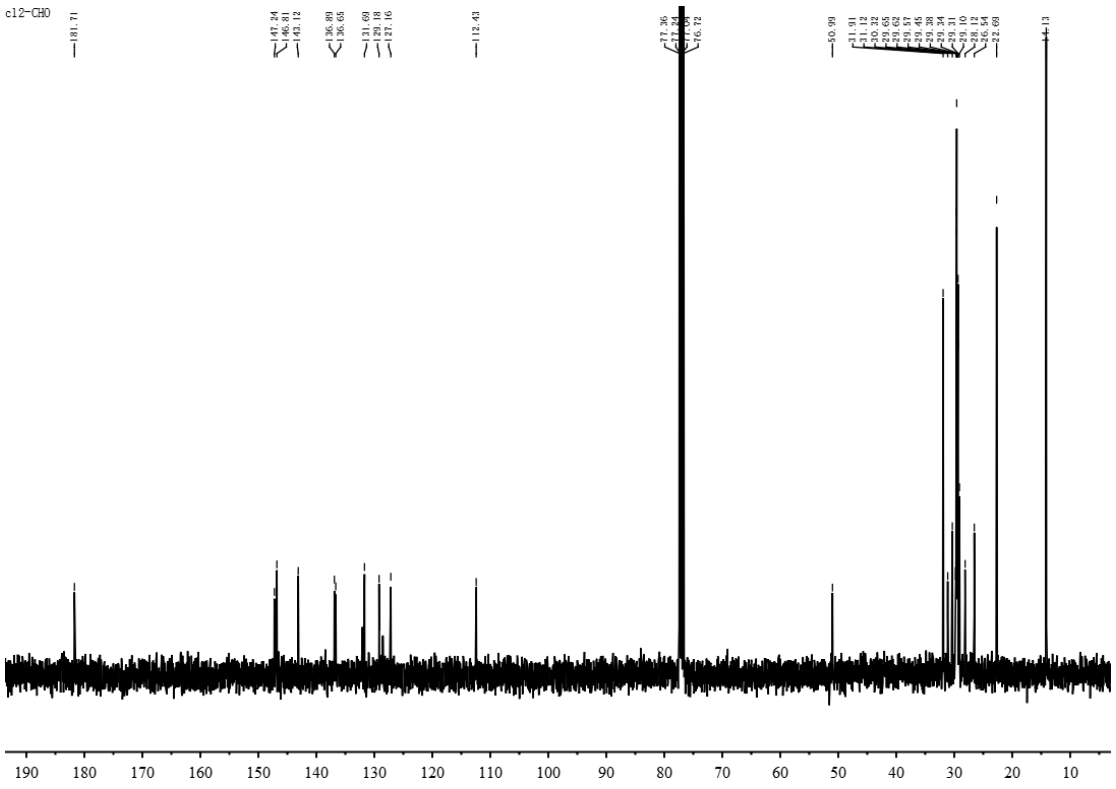

Figure S11. ^{13}C NMR spectrum of **4a** in $CDCl_3$.

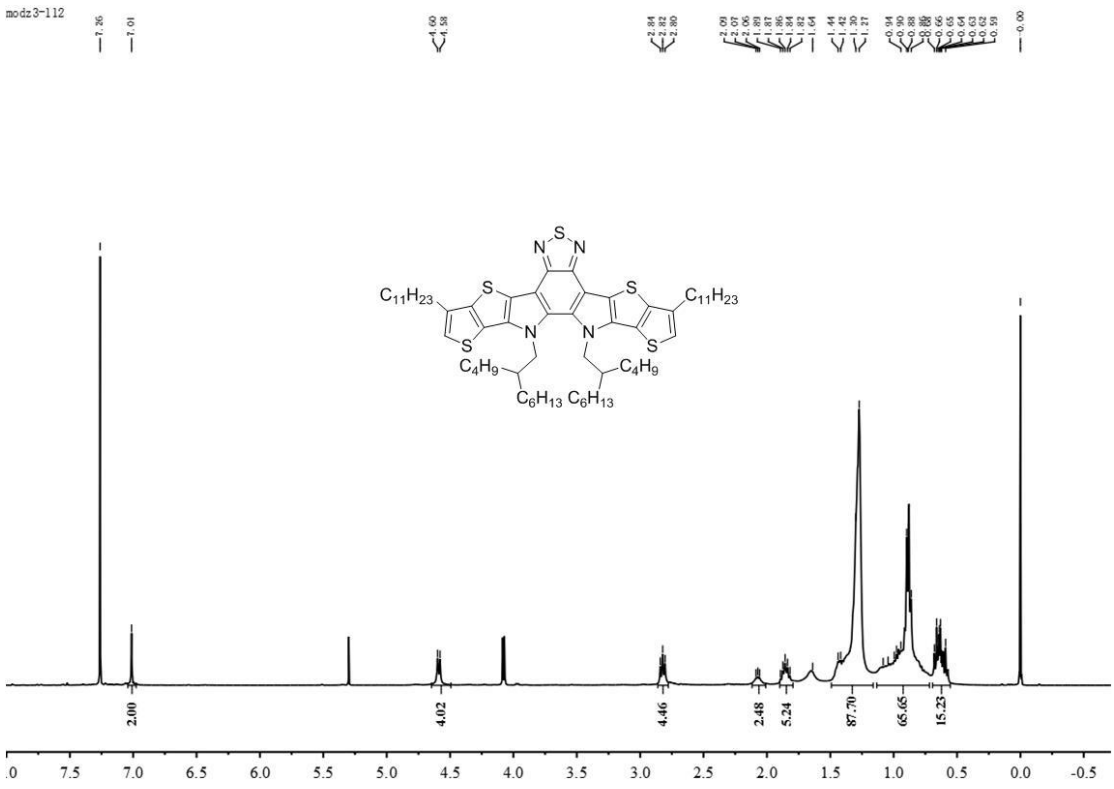

Figure S12. ^{1}H NMR spectrum of **3c** in $CDCl_3$.

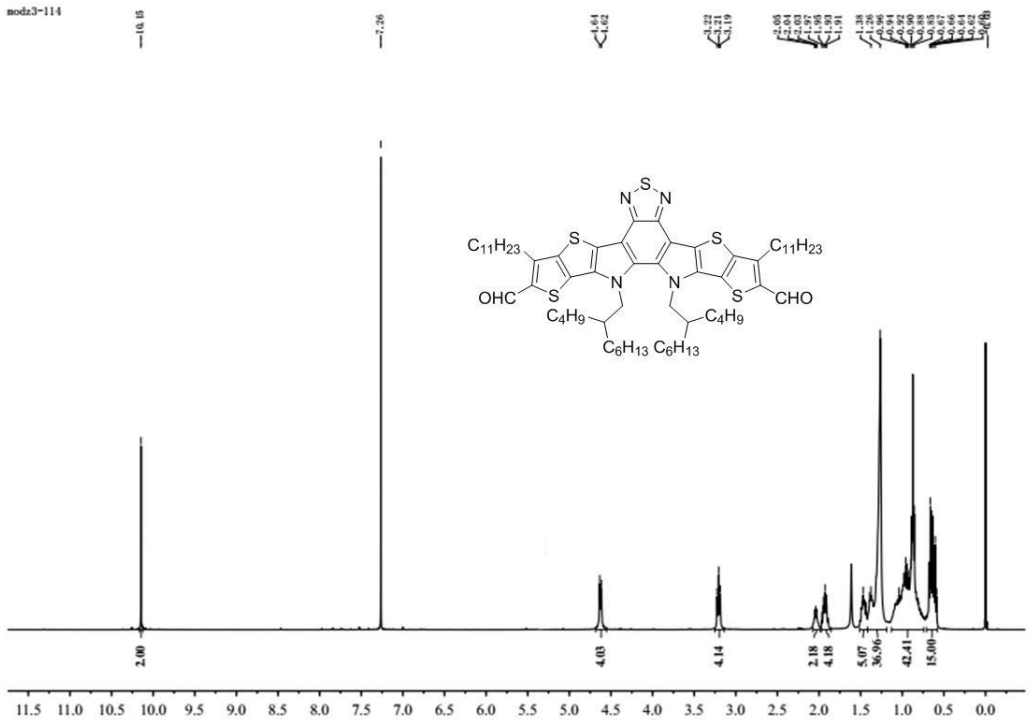

Figure S13. ^{1}H NMR spectrum of **4c** in $CDCl_3$.

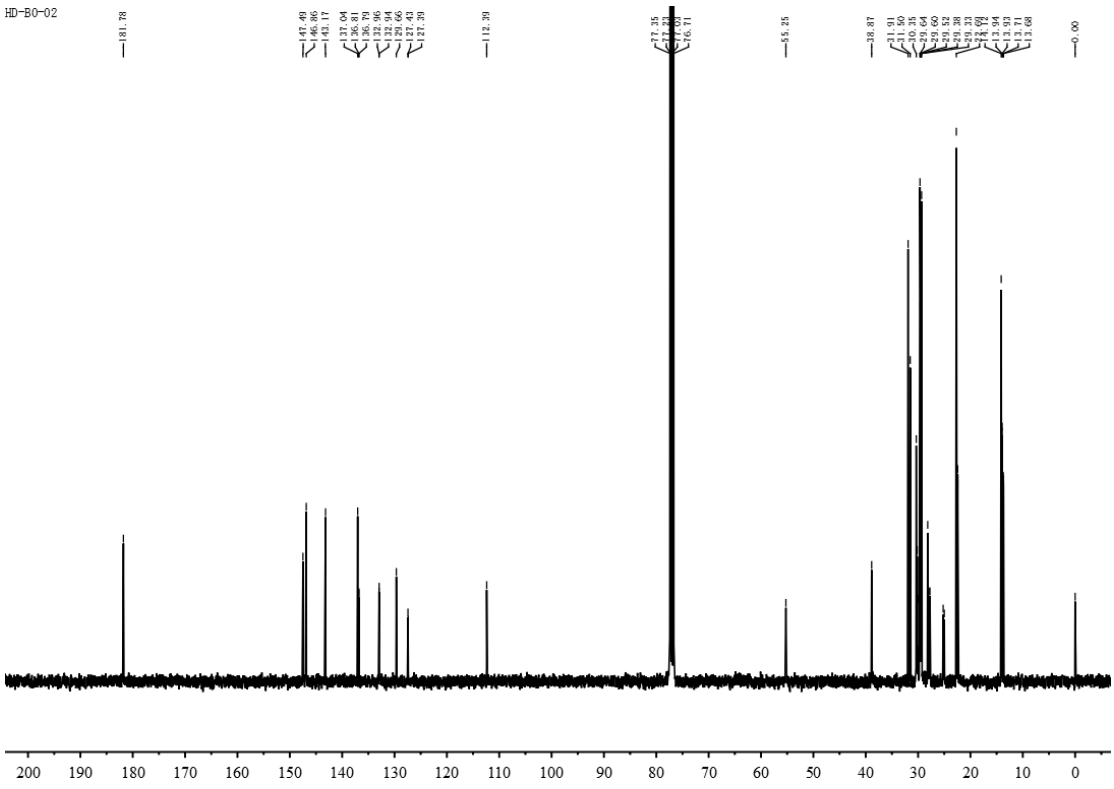

Figure S14. ^{13}C NMR spectrum of **4c** in $CDCl_3$.

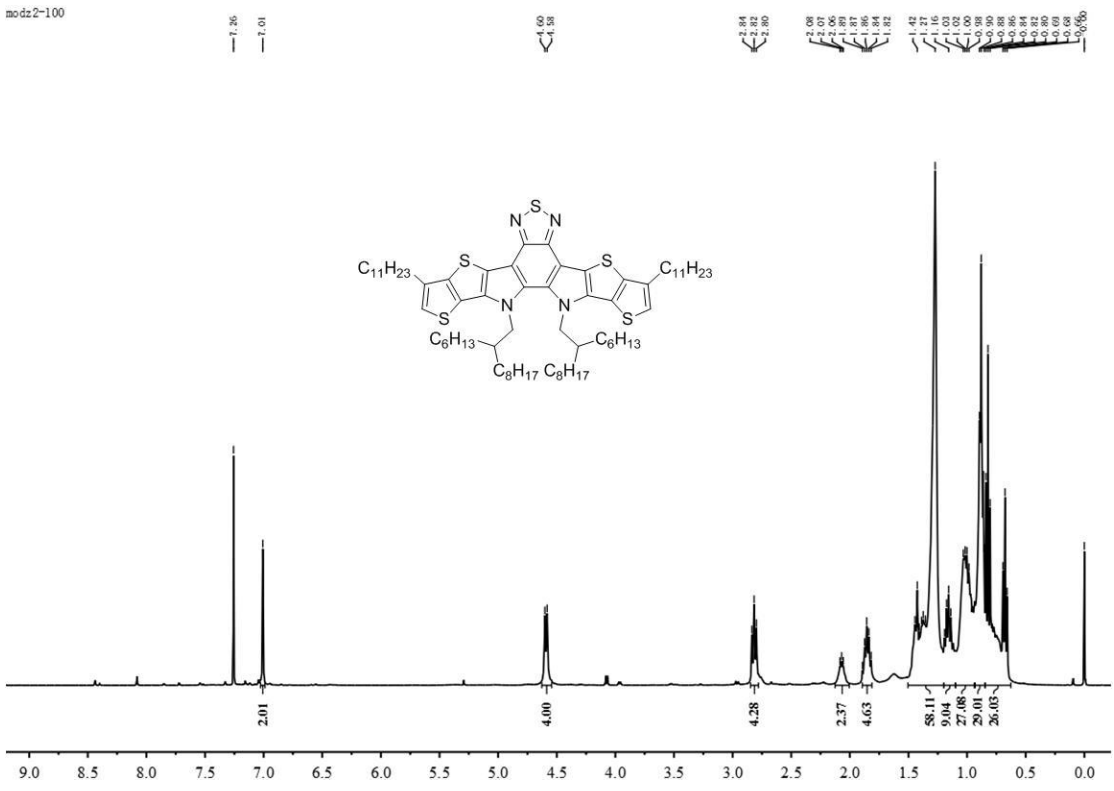

Figure S15. ^{1}H NMR spectrum of **3d** in $CDCl_3$.

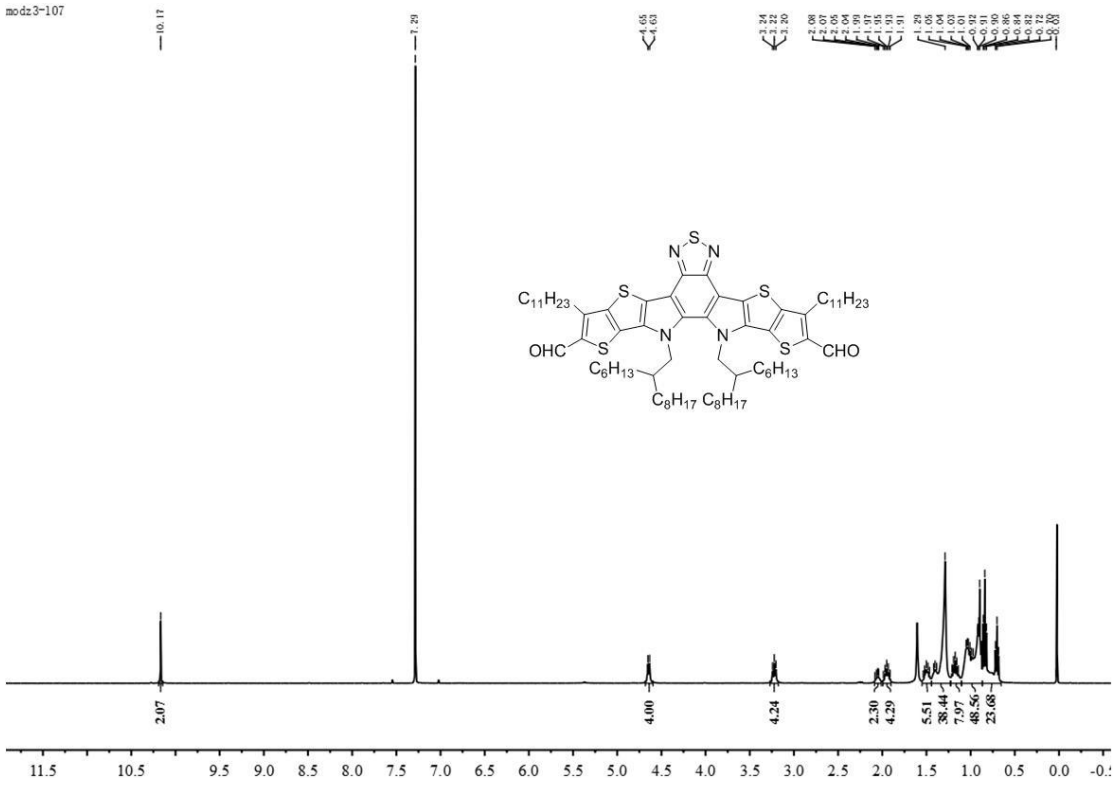

Figure S16. ^{1}H NMR spectrum of **4d** in $CDCl_3$.

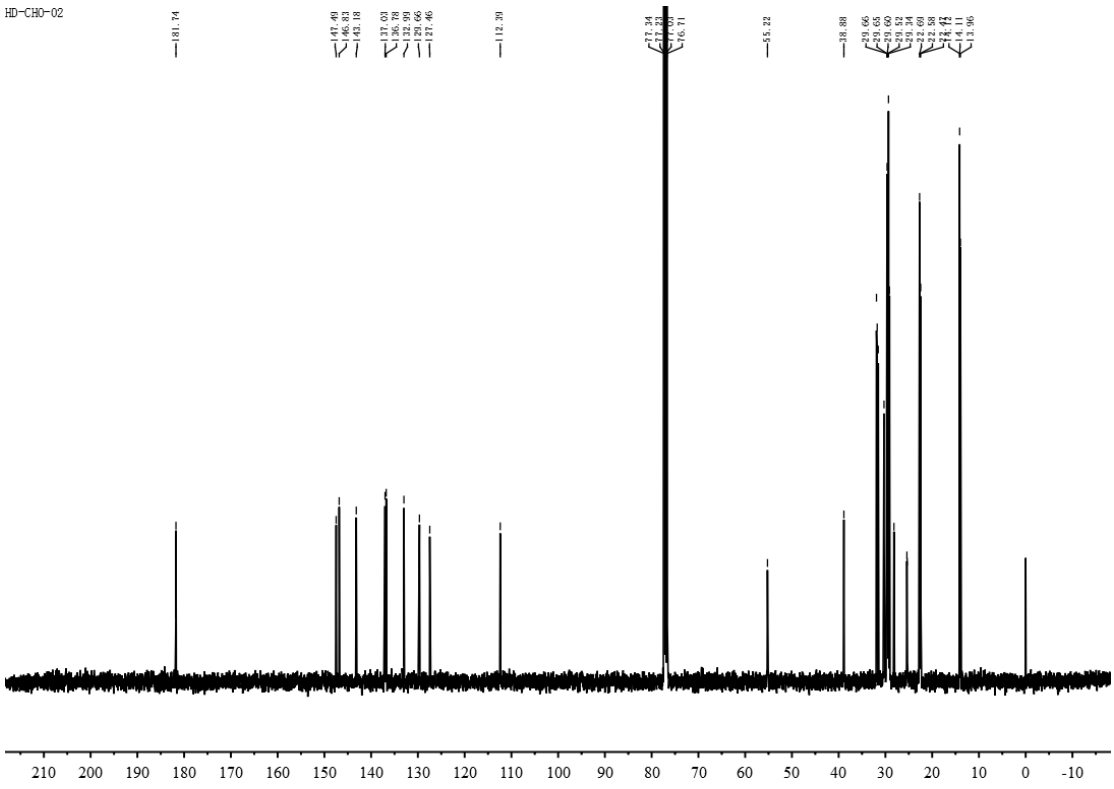

Figure S17. ^{13}C NMR spectrum of **4d** in $CDCl_3$.

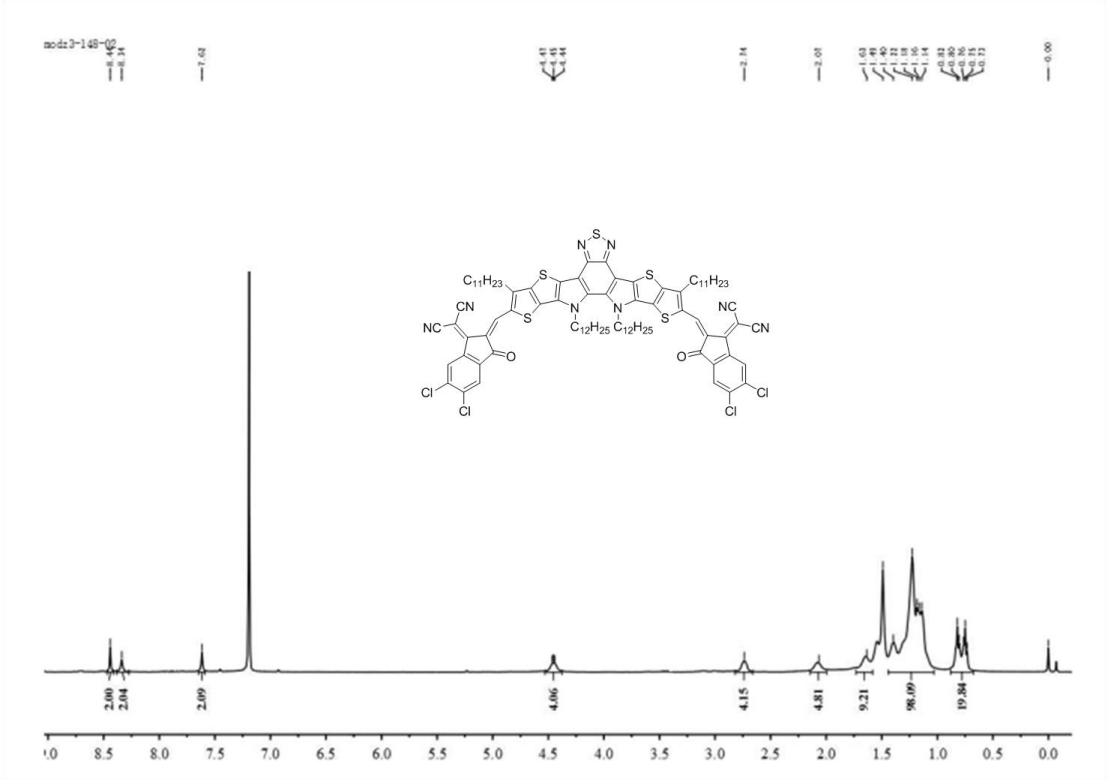

Figure S18. ^{1}H NMR spectrumof **5a** in $CDCl_3$.

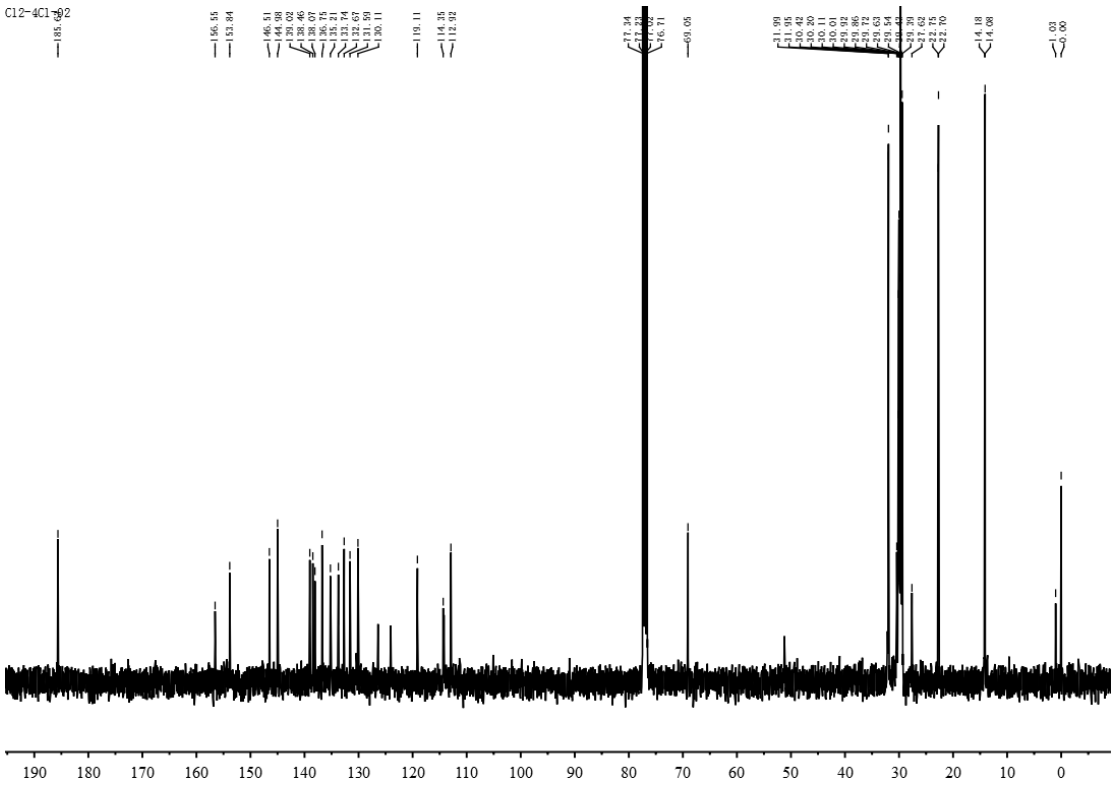

Figure S19. ^{13}C NMR spectrum of **5a** in $CDCl_3$.

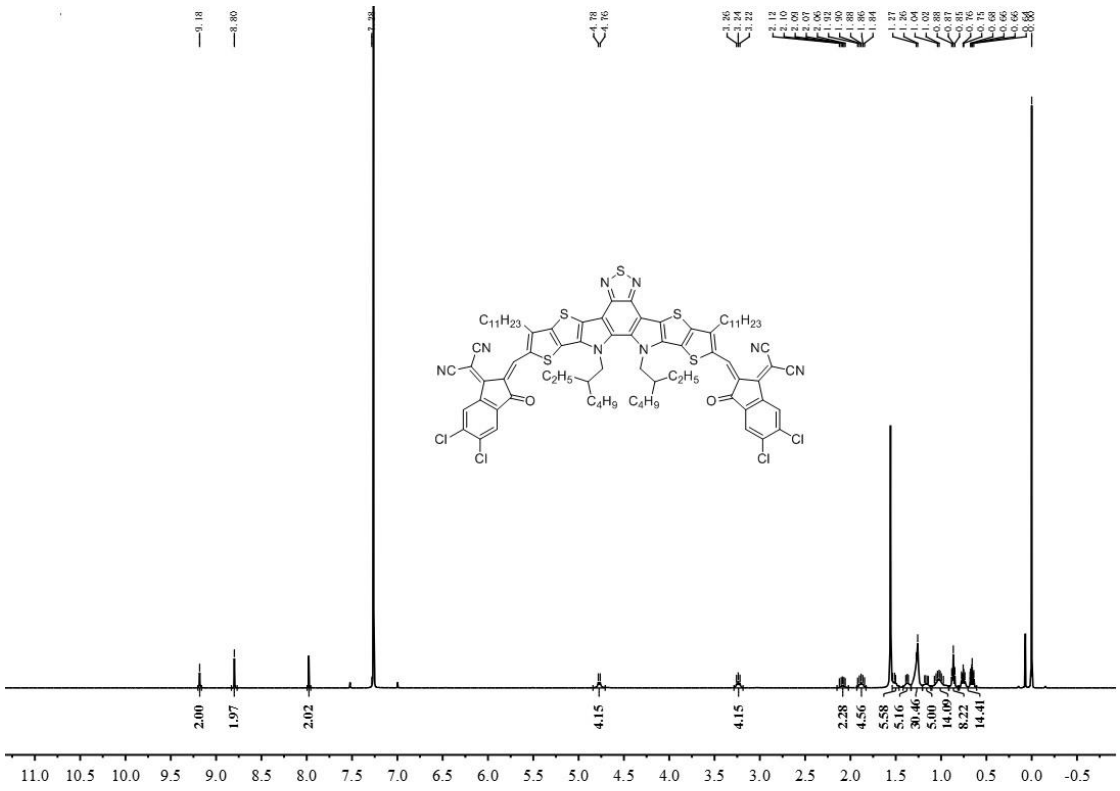

Figure S20. ^{1}H NMR spectrum of **5b** in $CDCl_3$.

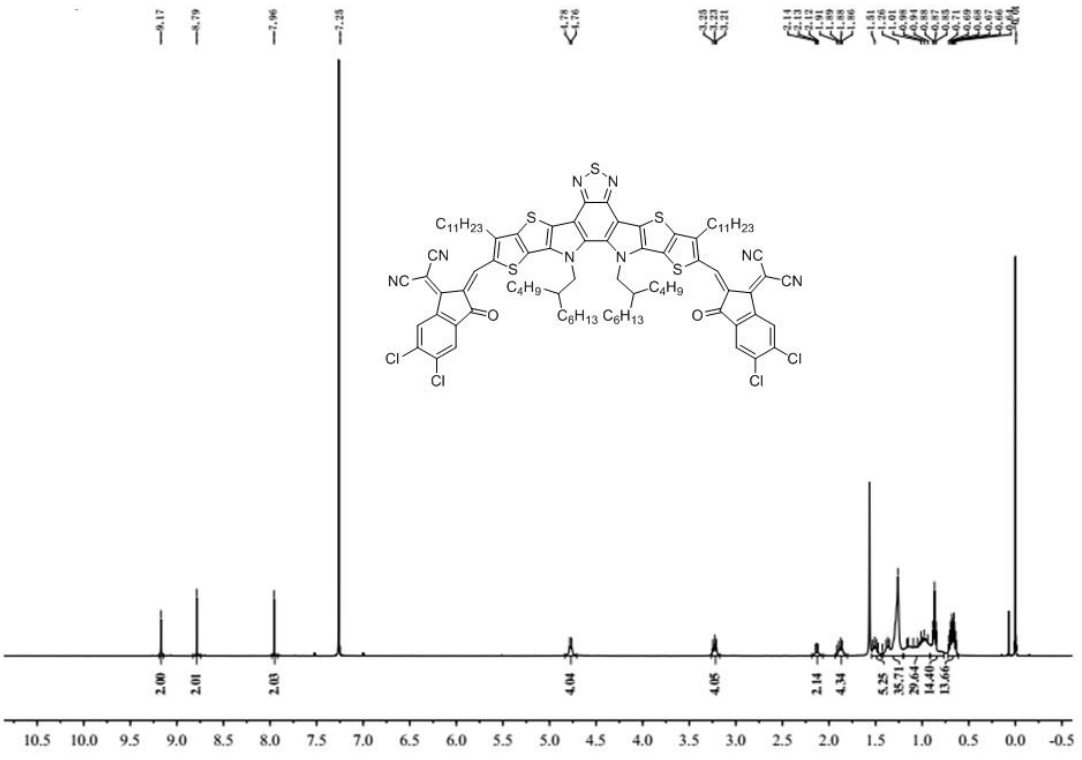

Figure S21. ^{1}H NMR spectrum of **5c** in $CDCl_3$.

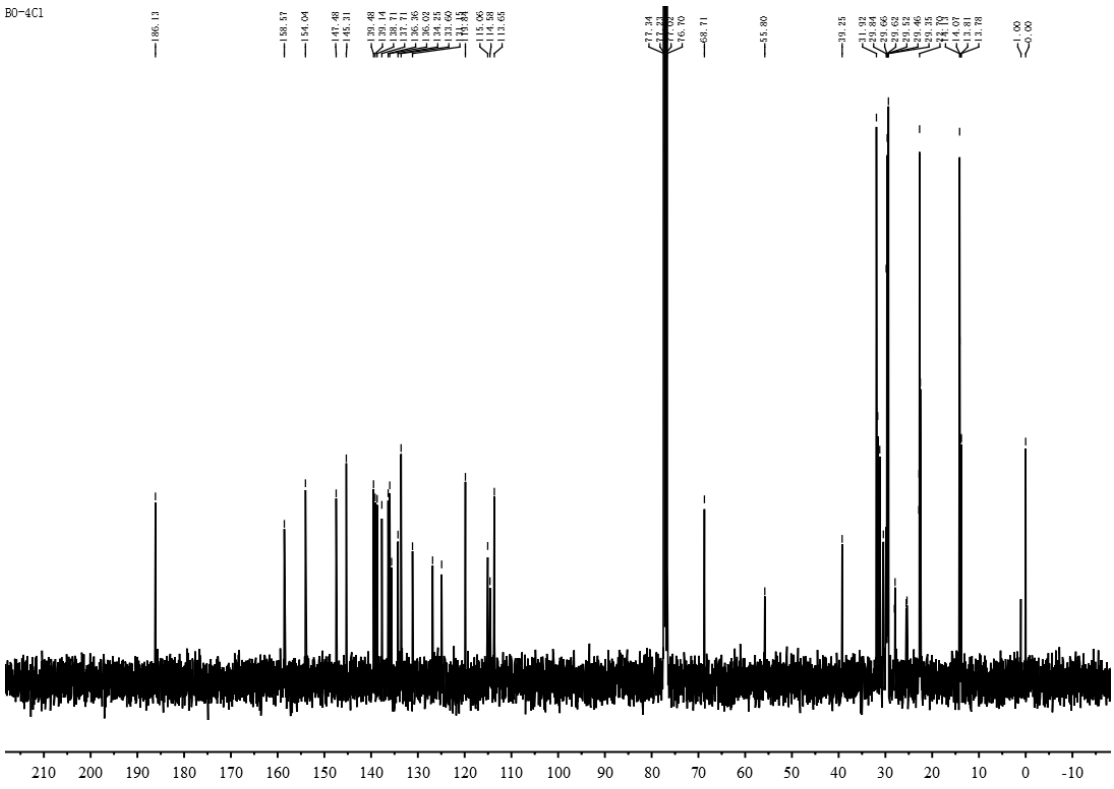

Figure S22. ^{13}C NMR spectrum of **5c** in $CDCl_3$.

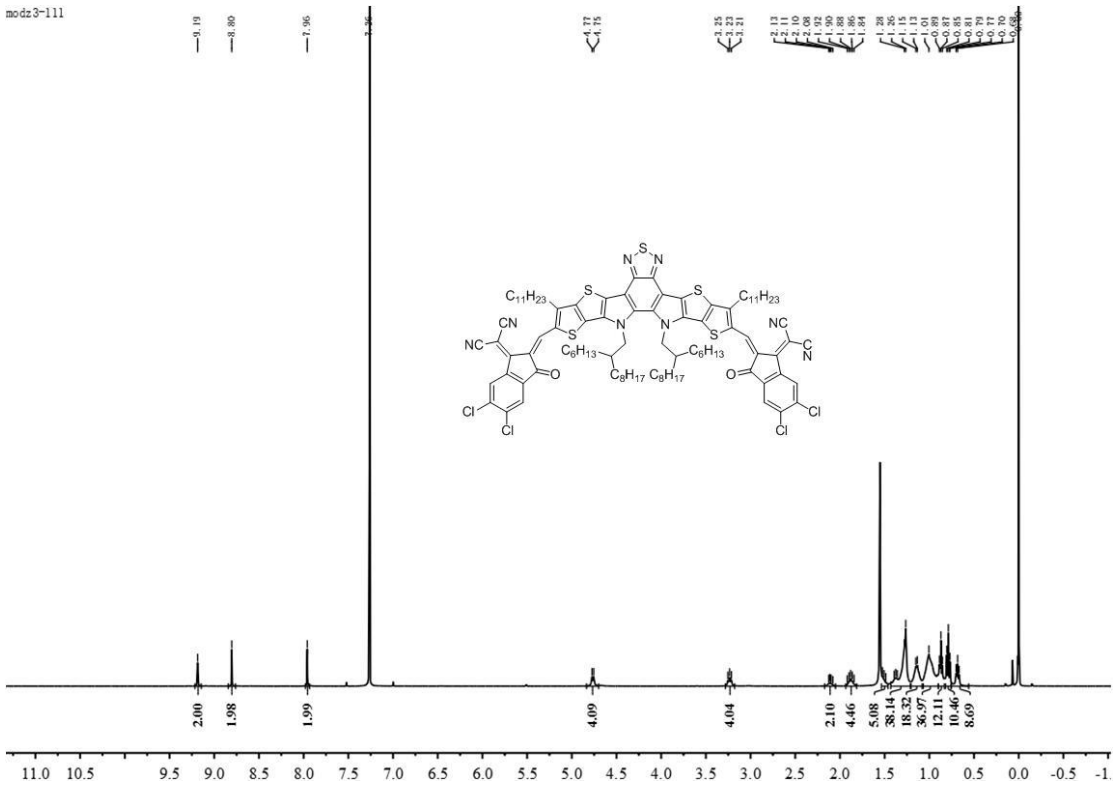

Figure S23. ^{1}H NMR spectrum of **5d** in $CDCl_3$.

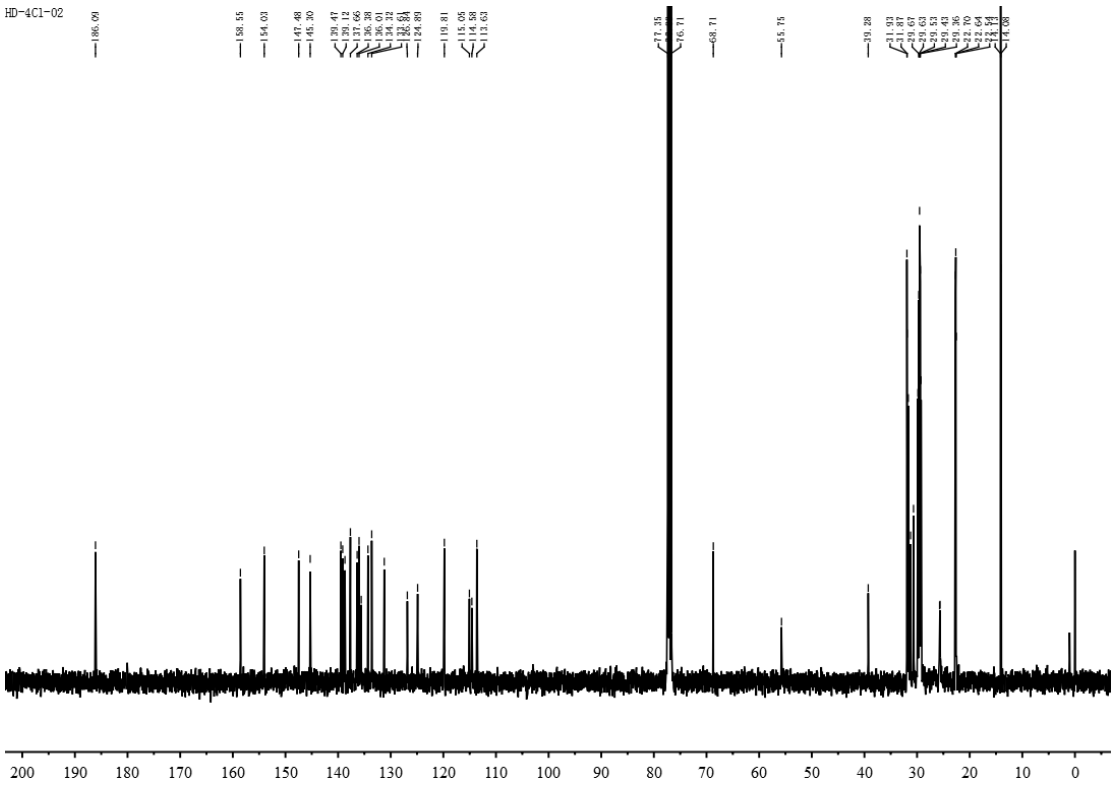

Figure S24. ^{13}C NMR spectrum of **5d** in $CDCl_3$.

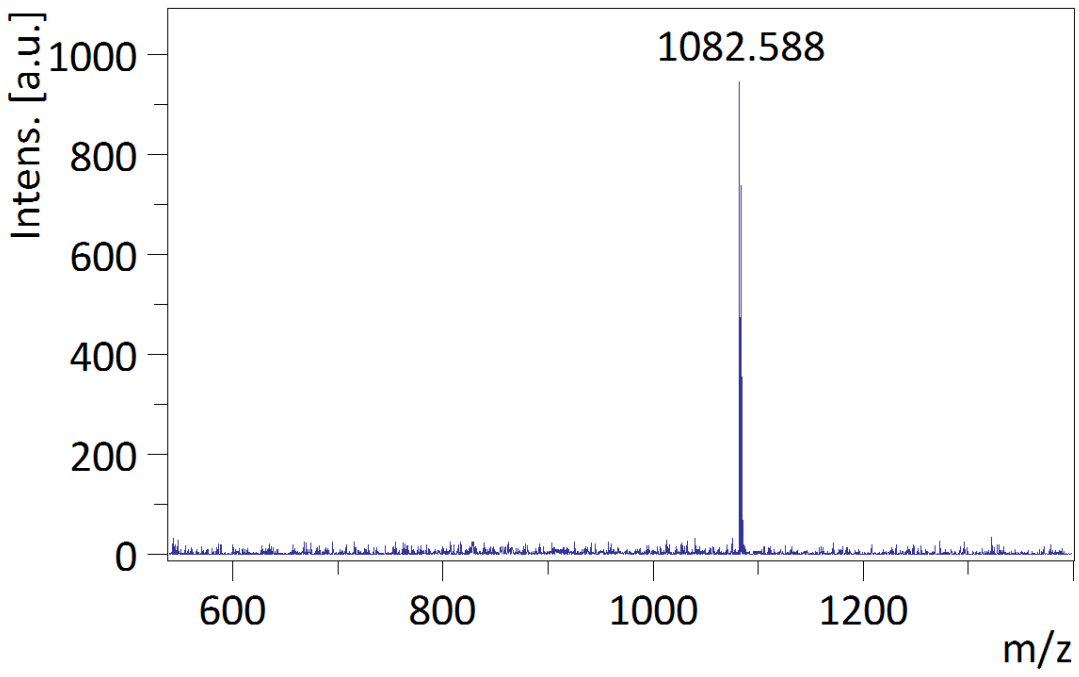

Figure S25. MS-MALDI spectrum of **3a**.

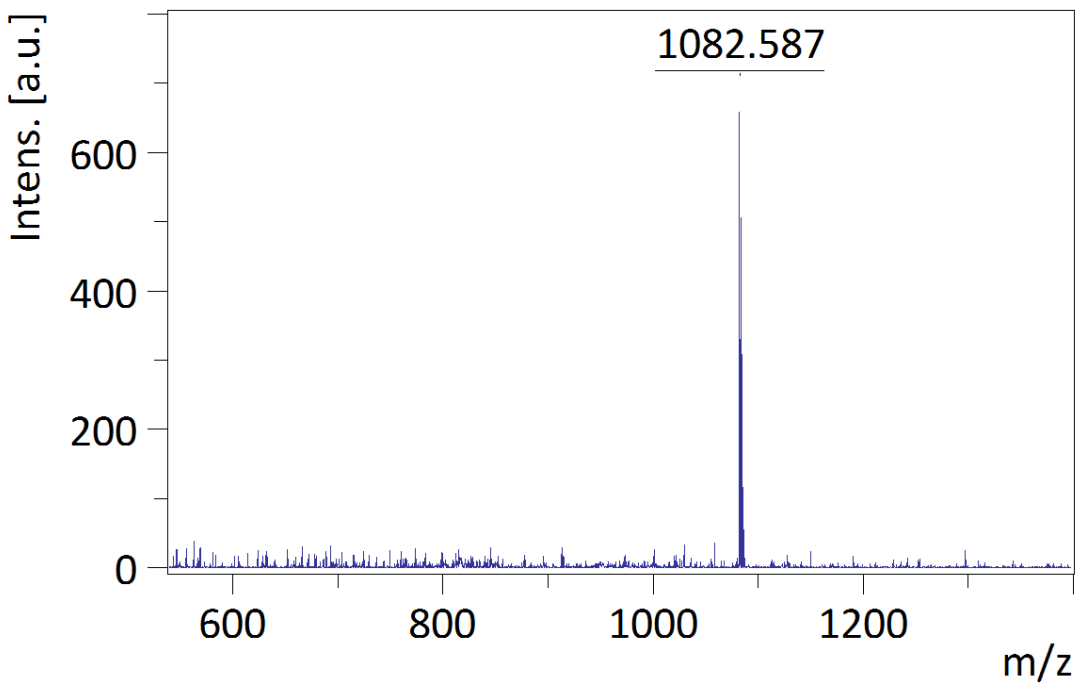

Figure S26. MS-MALDI spectrum of **3c**.

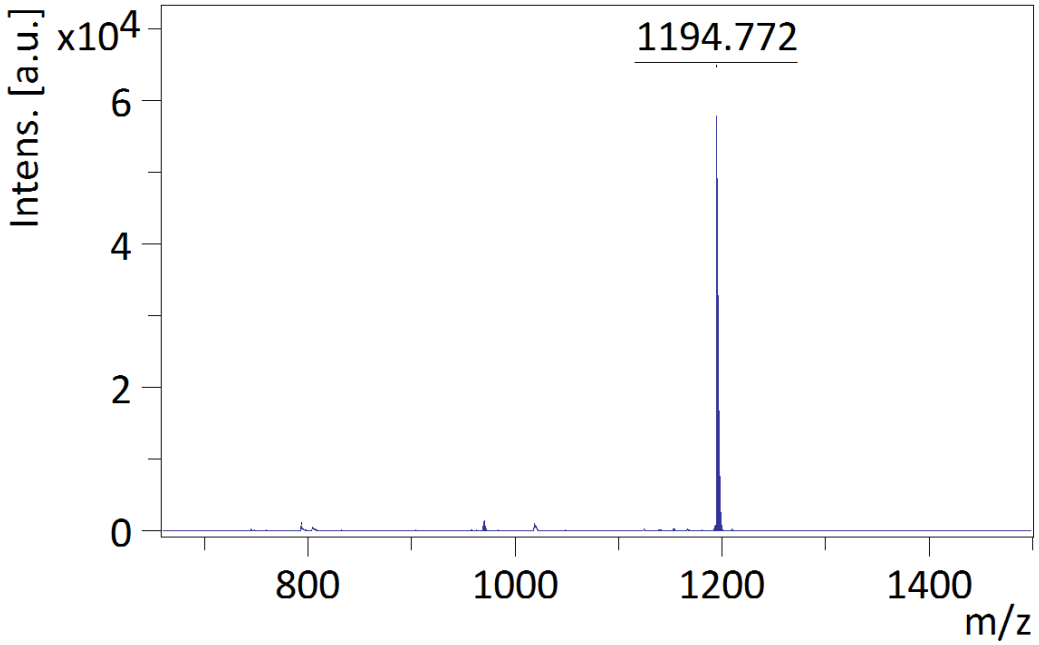

Figure S27. MS-MALDI spectrum of **3d**.

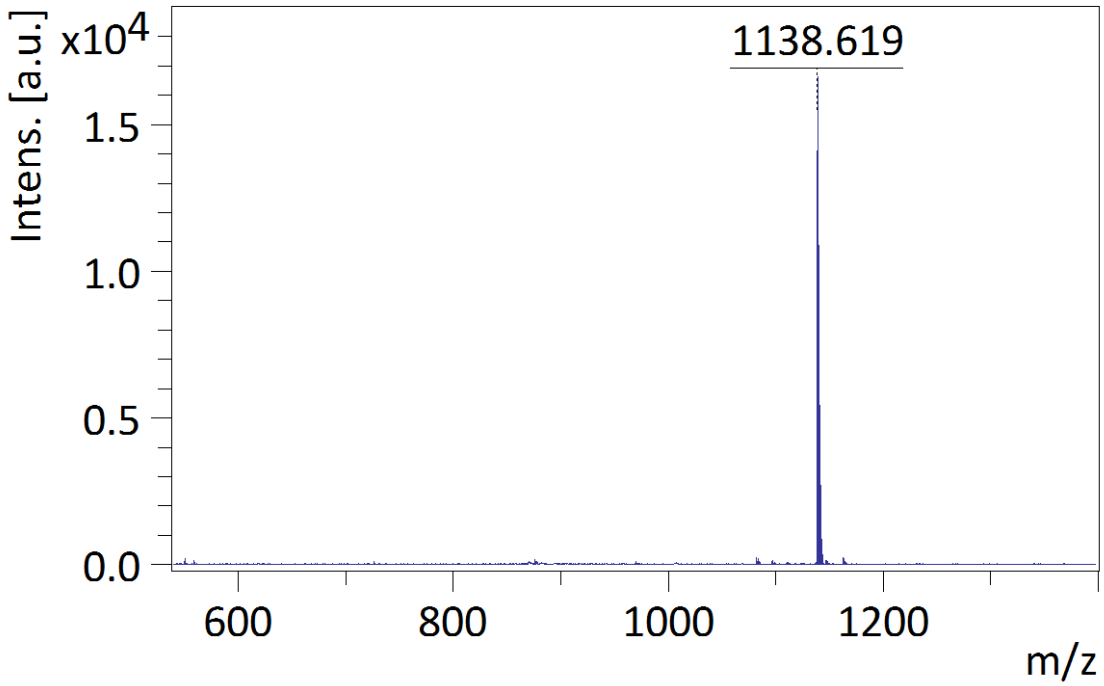

Figure S28. MS-MALDI spectrum of **4a**.

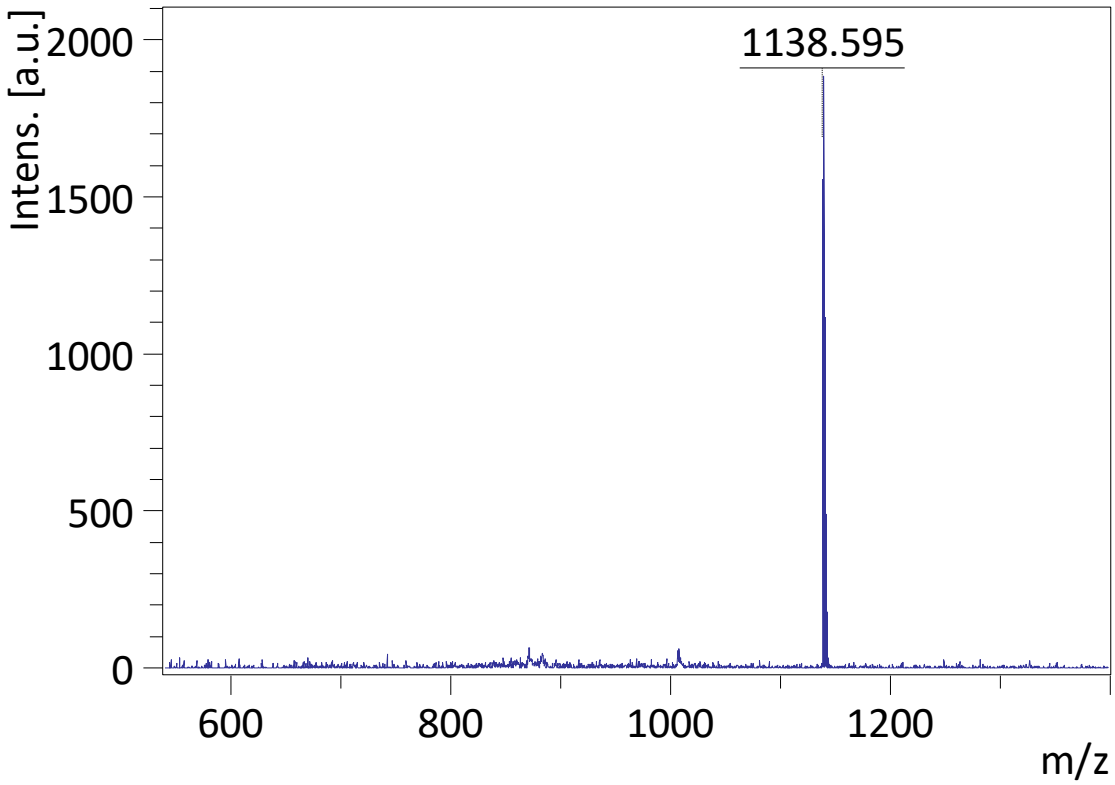

Figure S29. MS-MALDI spectrum of **4c**.

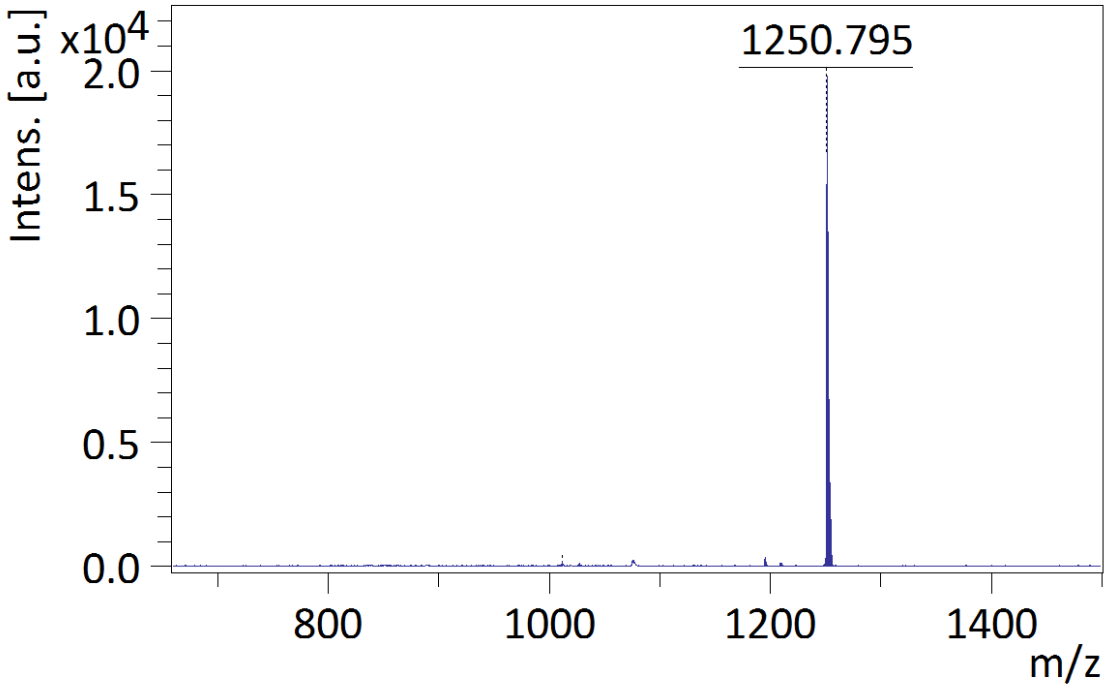

Figure S30. MS-MALDI spectrum of **4d**.

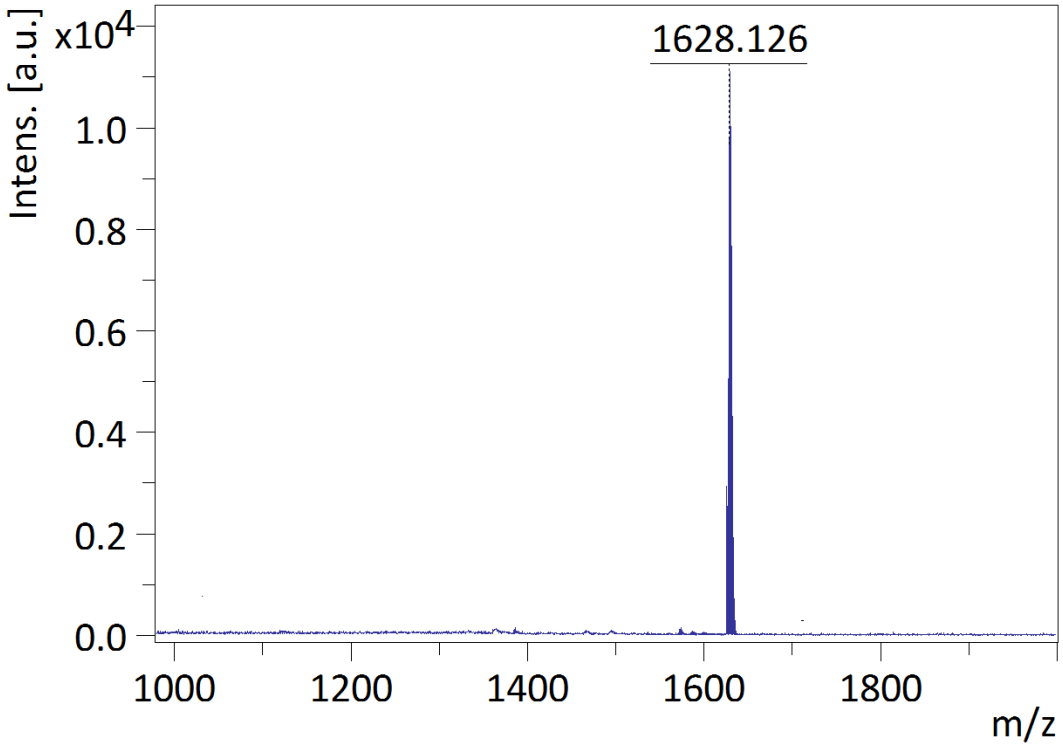

Figure S31. MS-MALDI spectrum of **BTIC-C12-4Cl**.

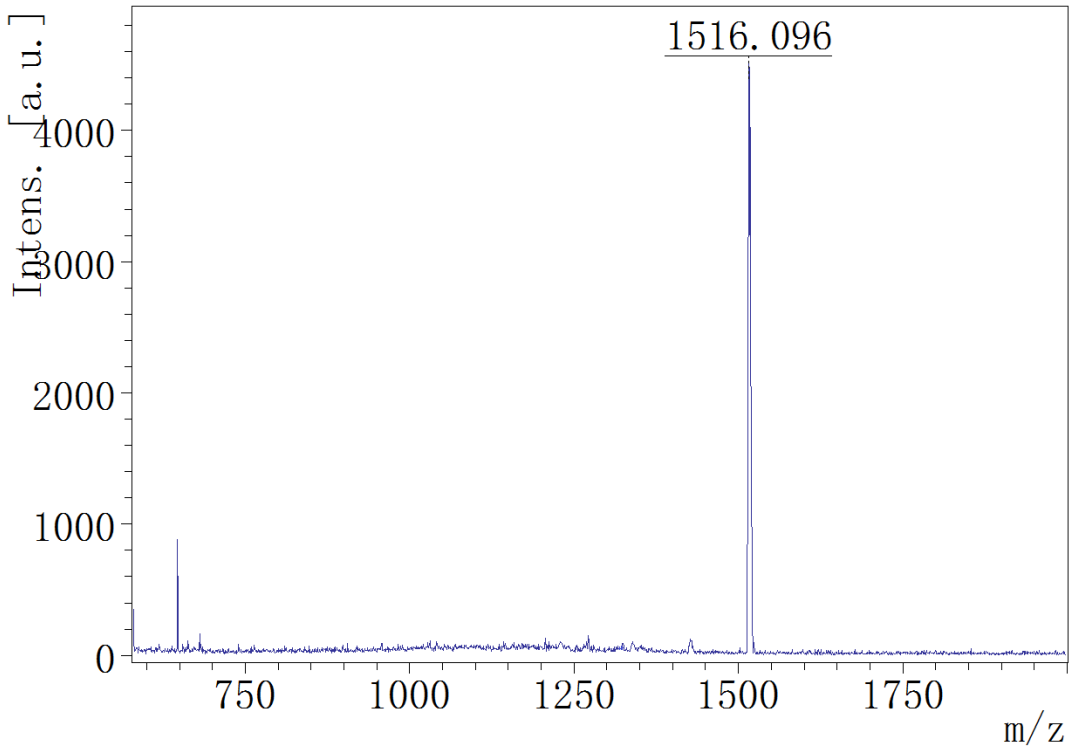

Figure S32. MS-MALDI spectrum of **BTIC-EH-4Cl**.

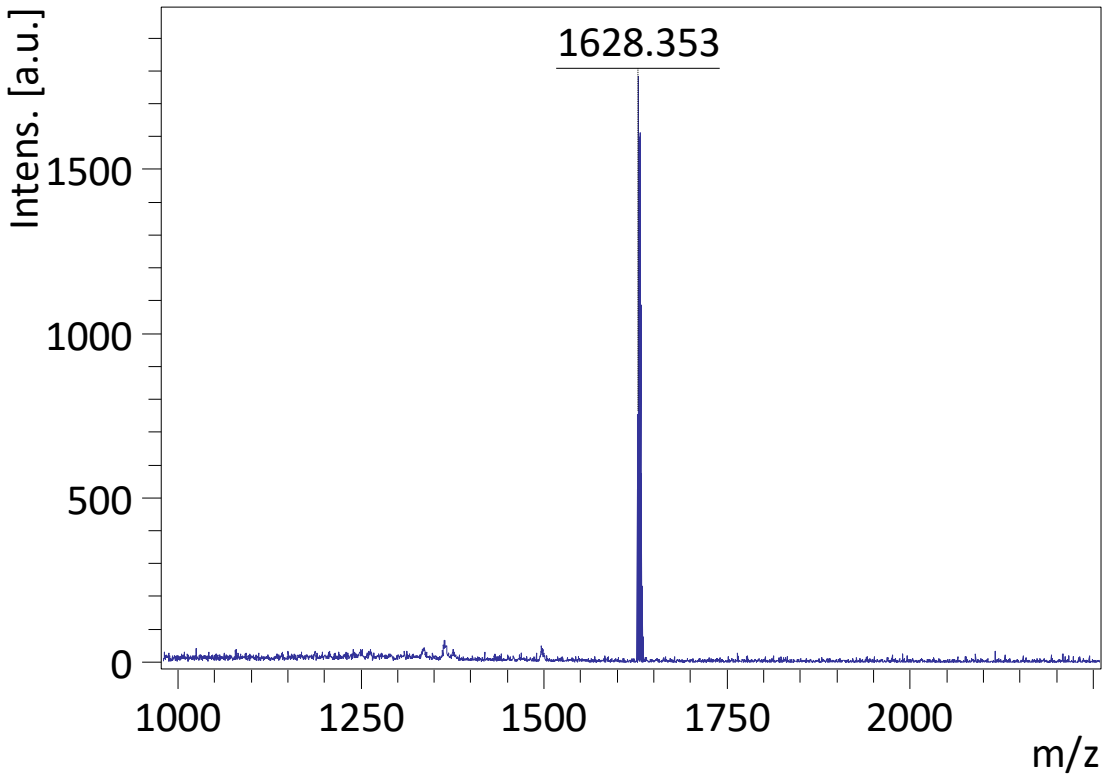

Figure S33. MS-MALDI spectrum of **BTIC-BO-4Cl**.

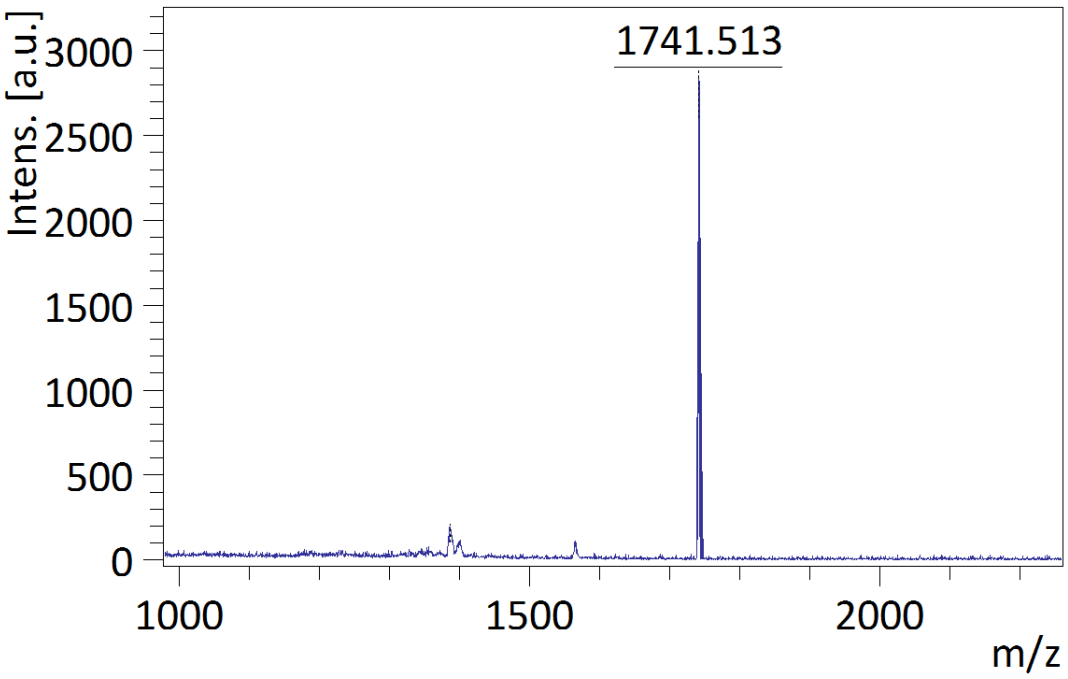

Figure S34. MS-MALDI spectrum of **BTIC-HD-4Cl**.